J|A|C|S COMMUNICATIONS

Published on Web 11/18/2009

Indium Tin Oxide Nanoparticles with Compositionally Tunable Surface Plasmon Resonance Frequencies in the Near-IR Region

Masayuki Kanehara,* Hayato Koike, Taizo Yoshinaga, and Toshiharu Teranishi*

Graduate School of Pure and Applied Sciences, University of Tsukuba, 1-1-1 Tennodai, Tsukuba, Ibaraki 305-8571, Japan

Received July 31, 2009; E-mail: kanehara@chem.tsukuba.ac.jp; teranisi@chem.tsukuba.ac.jp

Plasmonic nanostructures have attracted significant interest in recent years because of their potential applications in molecular-specific imaging and spectroscopy,[1,2] chemical and biological sensing,[3,4] biomedicine,[5,6] and nano-optical devices.[7,8] Most of the fundamental interest has focused on the size, shape, composition, and medium dependence of the surface plasmon resonance (SPR) in noble metals, especially gold and silver nanostructures.[9] This is because gold and silver nanostructures exhibit SPR frequencies in the visible−near-IR (vis−NIR) region, in contrast to their bulk plasma frequencies of 6.5 and 9.2 eV, respectively. On the other hand, a class of conducting metal oxides (CMOs) has plasma frequencies, ω_p, of <3 eV.[10,11] The SPRs for CMOs are phenomenologically the same as those observed in the noble metals, despite the fact that CMOs have lower charge carrier densities ($n \approx 10^{21}$ electrons/cm^3) than typical metals ($n \approx 10^{23}$ electrons/cm^3).[10−12] The SPR absorption wavelength, λ, is observed as presented in the following equation:

$$\lambda^2 = \lambda_p{}^2(\varepsilon^\infty + 2\varepsilon_m) \quad (1)$$

where λ_p is the material's bulk plasma wavelength, ε^∞ is the high-frequency dielectric constant, and ε_m is the dielectric constant of the surrounding medium. This equation explains the trends that the SPR absorption band is determined by the electron density of the SPR material and the refractive index of the surrounding medium.[13−15] By manipulation of these parameters, well-controlled SPRs of CMOs will contribute significantly in plasmon science applications because the use of expensive noble metals will no longer be required. A few studies of SPR of antimony-doped tin dioxide nanoparticles (NPs) have been reported,[16,17] but the synthesis of CMO NPs with controlled SPR properties is still a great challenge. Here we report the synthesis of conducting indium tin oxide (ITO) NPs and their SPR properties. The SPR peaks of the ITO NPs were easily tuned by changing the In/Sn molar ratio.

ITO NPs with different concentrations of Sn doping were readily synthesized by changing the In/Sn precursor ratios as follows. An *n*-octylether (10 mL) suspension of indium(III) acetate ($1.2 - x$ mmol), tin(II) 2-ethylhexanoate (x mmol), *n*-octanoic acid (3.6 mmol), and oleylamine (10 mmol) was stirred at 80 °C under vacuum for 30 min to form indium(III) octanoate. The solution was heated at 150 °C for 1 h under a N_2 atmosphere and stirred for a further 2 h at 280 °C to afford the ITO NPs. Repeated centrifugal purification by ethanol gave pure ITO NPs. The resulting ITO NPs were quite stable in toluene under ambient conditions for more than 1 year without changes in their optical absorption. As shown in Figure 1a−c, similar-sized ITO NPs with different mole percentages of Sn {%Sn = 100% × [Sn]/([Sn] + [In])} were successfully obtained. X-ray diffraction (XRD) analysis revealed that the %Sn in the ITO NPs could be controlled from 0 to 30% by changing the %Sn in the initial feeding from 0 to 40% (Figure 1d).

The crystal structures of all the ITO NPs were in good agreement with that of In_2O_3 NPs (Figure S1 in the Supporting Information),

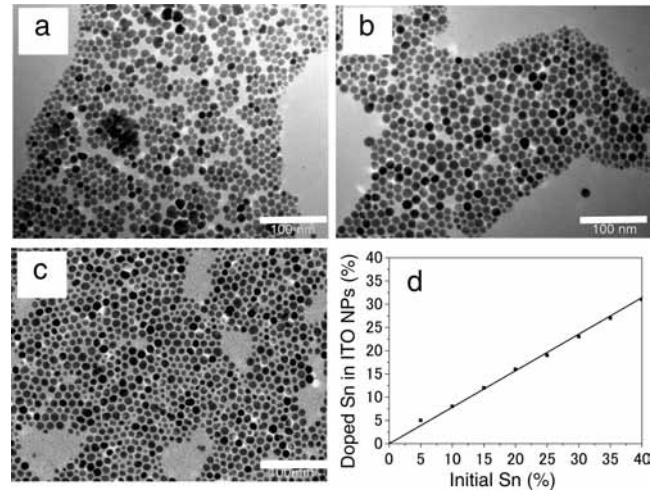

Figure 1. (a−c) TEM images of (a) In_2O_3 (11.3 ± 1.9 nm, 0% Sn), (b) ITO (12.8 ± 1.8 nm, 15% Sn) and (c) ITO (11.2 ± 1.8 nm, 30% Sn) NPs. The scale bars represent 100 nm. (d) Relationship between the %Sn in the initial feeding and the %Sn in the doped ITO NPs.

indicating that the In atoms were replaced by Sn atoms to form well-crystallized ITO NPs without formation of tin oxides such as SnO and SnO_2, which generate carrier traps at the grain boundaries to give lower carrier densities. Figure 2a,b shows the UV−vis−NIR spectra of ITO NPs with different %Sn. The ITO NPs had an interband transition at ∼400 nm and weak absorption in the red visible region, resulting in a faint bluish color. The In_2O_3 NPs did not show an SPR peak, whereas the ITO NPs showed clear SPR peaks from 1626 to >2200 nm. The SPR peak underwent a gradual blue shift from >2200 to 1618 nm as the %Sn increased from 3 to 10% (Figure 2a). Further doping of Sn into ITO NPs led to a gradual red shift of the SPR peak from 1626 to 1836 nm as the %Sn increased from 15 to 30% (Figure 2b). The NPs with shorter SPR wavelengths have higher free-electron densities, indicating that 10% Sn-doped ITO NPs have the highest electron density of the studied ITO NPs. These results are in good agreement with those for ITO thin films produced by a sol−gel process, where a 10% Sn-doped ITO film had both the highest electron density and the lowest resistivity.[18,19] In the electronic structure of an ITO crystal, a Sn atom that replaces an In atom gives a single free electron. Therefore, higher %Sn in the 0−10% range afforded higher free-electron density. However, further Sn doping leads to electron trapping around the Sn atoms, which decreases the electron density and gives a lower SPR frequency.[19] The SPR frequency is known to be affected by the refractive index of the surrounding medium. From Mie theory, plasmon material that is surrounded by a medium with a higher refractive index is expected to have a lower SPR frequency.[13,20] As expected, the ITO NPs in hexane, cyclohexane,

10.1021/ja9064415

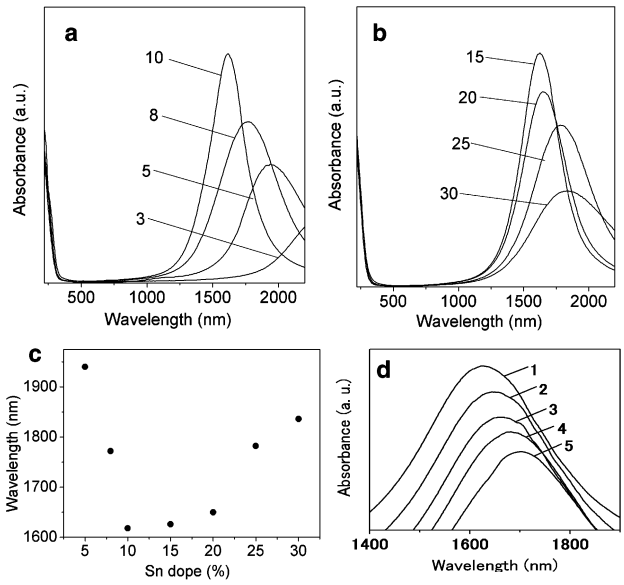

Figure 2. (a, b) UV−vis−NIR spectra of ITO NPs doped with (a) 3−10 and (b) 15−30% Sn. (c) Dependence of the SPR peaks of ITO NPs on the doped %Sn. The peak wavelengths of 5, 8, 10, 15, 20, 25, and 30% Sn-doped ITO NPs were 1940, 1772, 1618, 1626, 1650, 1782, and 1836 nm, respectively. (d) NIR spectra of 8% Sn-doped ITO NPs in (1) hexane (n = 1.37, 1626 nm), (2) cyclohexane (n = 1.42, 1646 nm), (3) decahydronaphthalene (n = 1.48, 1664 nm), (4) *o*-dichlorobenzene (n = 1.55, 1682 nm), and (5) nitrobenzene (n = 1.55, 1702 nm). The refractive indexes of the solvents (n) and peak wavelengths are given in the parentheses.

decahydronaphthalene, *o*-dichlorobenzene, and nitrobenzene showed different SPR peaks, reflecting the refractive indexes of the solvents (Figure 2d). Despite the same refractive indexes of *o*-dichlorobenzene and nitrobenzene, different SPR peaks were observed because of the polarity of the nitro group, which interacts strongly with the ITO NP surfaces to change the SPR frequency.

The ITO NPs could be used to form a densely packed ITO NP film on a glass substrate. The 5 wt % toluene solution of 8% Sn-doped ITO NPs was spin-coated onto a glass substrate to form the ITO NP film with a 50 nm thickness. The SPR peak was red-shifted from 1772 nm in the toluene solution to 1996 nm in the ITO film, indicating the SPR coupling between the neighboring ITO NPs (Figure S2).[21,22] The ITO film was subsequently annealed at 600 °C under air for 30 min to remove the organic ligand layer. Thermogravimetric analysis revealed that the ligand layer of the ITO NPs was perfectly removed by annealing at 415 °C under air. After the ITO film was annealed, its SPR peak was significantly reduced, reflecting the decrease in the free-electron density. In addition to the electron carrier generated by the doped Sn, oxygen defects (i.e., two electron carriers) play an important role in electric conductivity. The electron conductivity of an ITO film is well-known to be significantly reduced by oxidative annealing as a result of oxidation of the oxygen defects to give a lower electron carrier density.[23,24] The oxygen defects can be regenerated by reductive annealing under an H_2 atmosphere, and this method could also be applied to our ITO film. After the ITO NP film was annealed under 4% H_2/Ar at 450 °C for 30 min, the SPR peak was regenerated at 2392 nm. The red shift by 396 nm from that of the spin-coated ITO NP film shows stronger SPR coupling resulting from a reduction of the interparticle spacing of the ITO NPs. XRD measurements revealed that the crystalline diameter of the ITO NPs was maintained after these annealing processes, and these results also support the finding that the red shift of the SPR is not derived from an agglomeration but the SPR coupling between the ITO NPs (Figure S3).

In conclusion, we have demonstrated that the SPR peaks of ITO NPs can be tuned by controlling the electron carrier densities. The SPR absorption of ITO NPs was easily controlled from 1618 to >2200 nm by changing the concentration of the Sn doping from 3 to 30 mol %. The shortest SPR wavelength at 1618 nm in the 10% Sn-doped ITO NPs may reflect the highest electron carrier density among the studied ITO NPs. This is the first example of well-defined SPR-tunable conductive metal oxide NPs in the NIR region. While gold is easily electrochemically oxidized, ITO can withstand voltages of >1000 V in solution or polymer films. This indicates the excellent stability of the ITO. Unlike noble-metal nanostructures, ITO has no inter- and intraband transitions in the vis−NIR region and represents a free-electron conduction, allowing us to systematically study the origin of the optical effects arising from the SPR of conduction electrons.

Acknowledgment. The present work was supported by a Grant-in-Aid for Scientific Research on Priority Area "Strong Photon-Molecule Coupling Fields" (No. 470) (19049007) and a Grant-in-Aid for Scientific Research (A) (19205016) from MEXT, Japan (T.T.).

Supporting Information Available: XRD patterns of ITO NPs and UV−vis−NIR spectra and XRD patterns of ITO NP films. This material is available free of charge via the Internet at http://pubs.acs.org.

References

(1) Ohko, Y.; Tatsuma, T.; Fujii, T.; Naoi, K.; Niwa, C.; Kubota, Y.; Fujishima, A. *Nat. Mater.* **2002**, *2*, 29.
(2) El-Sayed, I. H.; Huang, X.; El-Sayed, M. A. *Nano Lett.* **2005**, *5*, 829.
(3) Novo, C.; Funston, A. M.; Mulvaney, P. *Nat. Nanotechnol.* **2008**, *3*, 598.
(4) Rosi, N. L.; Mirkin, C. A. *Chem. Rev.* **2005**, *105*, 1547.
(5) Loo, C.; Lowery, A.; Halas, N.; West, J.; Drezek, R. *Nano Lett.* **2005**, *5*, 709.
(6) Huang, X.; El-Sayed, I. H.; Qian, W.; El-Sayed, M. A. *J. Am. Chem. Soc.* **2006**, *128*, 2115.
(7) Maier, S. A.; Brongersma, M. L.; Kik, P. G.; Meltzer, S.; Requicha, A. A. G.; Atwater, H. A. *Adv. Mater.* **2001**, *13*, 1501.
(8) Volkov, V. S.; Bozhevolnyi, S. I.; Rodrigo, S. G.; Martín-Moreno, L.; García-Vidal, F. J.; Devaux, E.; Ebbesen, T. W. *Nano Lett.* **2009**, *9*, 1278.
(9) Odom, T. W.; Nehl, C. L. *ACS Nano* **2009**, *2*, 612.
(10) Franzen, S. *J. Phys. Chem. C* **2008**, *112*, 6027.
(11) Rhodes, C.; Franzen, S.; Maria, J.-P.; Losego, M.; Leonard, D. N.; Laughlin, B.; Duscher, G.; Weibel, S. *J. Appl. Phys.* **2006**, *100*, 054905.
(12) Losego, M. D.; Efremenko, A. Y.; Rhodes, C. L.; Cerruti, M. G.; Franzen, S.; Maria, J.-P. *J. Appl. Phys.* **2009**, *106*, 024903.
(13) Underwood, S.; Mulvaney, P. *Langmuir* **1994**, *10*, 3427.
(14) Mulvaney, P. *Langmuir* **1996**, *12*, 788.
(15) Mulvaney, P. In *Semiconductor Nanoclusters: Physical, Chemical and Catalytic Aspects*; Kamat, P. V., Meisel, D., Eds.; Elsevier Science: Amsterdam, 1997; p 99.
(16) Nütz, T.; zum Felde, U.; Haase, M. *J. Chem. Phys.* **1999**, *110*, 12142.
(17) zum Felde, U.; Haase, M.; Weller, H. *J. Phys. Chem. B* **2000**, *104*, 9388.
(18) Alam, M. J.; Cameron, D. C. *Thin Solid Films* **2000**, *377−378*, 455.
(19) Kima, S.-S.; Choi, S.-Y.; Park, C.-G.; Jin, H.-W. *Thin Solid Films* **1999**, *347*, 155.
(20) Shi, W.; Zeng, H.; Sahoo, Y.; Ohulchanskyy, T. Y.; Ding, Y.; Wang, Z. L.; Swihart, M.; Prasad, P. N. *Nano Lett.* **2006**, *6*, 875.
(21) Lassiter, J. B.; Aizpurua, J.; Hernandez, L. I.; Brandl, D. W.; Romero, I.; Lal, S.; Hafner, J. H.; Nordlander, P.; Halas, N. J. *Nano Lett.* **2008**, *8*, 1212.
(22) Chen, C.-F.; Tzeng, S.-D.; Chen, H.-Y.; Lin, K.-J.; Gwo, S. *J. Am. Chem. Soc.* **2008**, *130*, 824.
(23) Low, B.; Zhu, F.; Zhang, K.; Chua, S. *Appl. Phys. Lett.* **2002**, *80*, 4659.
(24) Kim, S. Y.; Lee, J.-L.; Kim, K.-B.; Tak, Y.-H. *J. Appl. Phys.* **2004**, *95*, 2560.

JA9064415